Photochemistry and Photobiology, 2006, 82: 13–19

Diastereoselectivity and Site Dependency in the Photochemistry of Ketoprofen in the Bovine Serum Albumin Matrix†

Sandra Monti*[1], Ilse Manet[1], Francesco Manoli[1], Raffaele Morrone[2], Giovanni Nicolosi[2] and Salvatore Sortino[3]

[1]Istituto per la Sintesi Organica e la Fotoreattività (ISOF), CNR, Via P. Gobetti 101, 40129 Bologna, Italy
[2]Istituto di Chimica Biomolecolare—Sezione di Catania, Via del Santuario 110, 95028 Valverde (CT) Italy
[3]Dipartimento di Scienze Chimiche, Università di Catania, Viale A. Doria 8, 95125 Catania, Italy

Received 11 July 2005; accepted 22 September 2005; published online 27 September 2005 DOI: 10.1562/2005.07-11-RA-608

ABSTRACT

The photodegradation of the S(+)- and R(−)-ketoprofen (KP) enantiomers in the bovine serum albumin matrix was studied by steady-state photolysis with the use of λ_{irr} > 320 nm and transient absorption spectroscopy with λ_{exc} = 355 nm, at 1/1 and 2/1 KP/BSA molar ratios. R(−)-KP was found to be more labile than S(+). Triplet ketoprofen species were evidenced with lifetimes of 400 ns for S(+) and 600 ns for R(−)-KP. Further longer-lived transients with lifetimes of 2.6 and 6.0 μs for S(+) and R(−), respectively, were detected. On the basis of the binding constants of the drug enantiomers to the two main binding sites of the protein, obtained from circular dichroism experiments, the individual disappearance quantum yields of the 1:1 and 2:1 diastereomeric KP:BSA complexes could be estimated. The photoreactivity in the BSA matrix was rationalized on the basis of diastereoselective photodecarboxylation in the two main protein sites.

INTRODUCTION

Ketoprofen (KP) is a nonsteroidal antinflammatory drug (NSAID) capable of inducing adverse photosensitizing reactions (1,2). Such undesired effects are due to the substituted benzophenone chromophore, which under UVA light generates noxious intermediates and photoproducts able to attack biological cell substrates. The environment strongly influences the photochemistry of KP: In a neutral aqueous medium a very efficient excited-state decarboxylation (Φ = 0.75) occurs, leading to 3-ethylbenzophenone as the main photoproduct in anaerobic conditions (3–6); in the β-cyclodextrin cavity the photofragmentation is strongly suppressed and an H-abstraction pathway becomes active, leading to reduction of the aromatic carbonyl with formation of adducts to the macrocycle (7) (see Scheme 1). The photobehavior of KP in cyclodextrin cavities can be considered a model for that in protein matrices, where covalent photobinding is at the basis of both photoaffinity labeling applications (8,9) and adverse production of photoantigens in therapy (10,11).

The role of stereospecific interactions in the photochemical reactions of KP in protein matrices has received little attention up to now. To the best of our knowledge, this matter, also important for the pharmacokinetic profile of the drug, which is active only as S(+) enantiomer (12), has been the object of only one study, in which the photodegradation of both KP enantiomers was examined in the bovine serum albumin (BSA) and human serum albumin (HSA) matrices (13). Decarboxylation was indicated to be the main photoreaction, occurring with quantum yields considerably lower than in water; BSA was shown to exhibit the best discriminating properties, providing a quantum yield for R(−)-KP degradation about 40% higher than that for S(+)-KP at KP/BSA molar ratio of 1.27.

We have recently examined the chiral recognition of KP enantiomers by BSA with the use of circular dichroism (CD) and fluorescence (14). This study, performed in the KP/BSA molar ratio range from 0.4 to 2.2, evidenced enantioselective binding and allowed us to achieve a characterization of the two main protein-binding sites for each enantiomer. No differences were found in the association constants of the two enantiomers, but well-defined and distinct CD spectra were determined for both the 1/1 and the 2/1 KP/BSA diastereomeric complexes. In light of the new information gained, the photochemistry of KP within the BSA matrix was worth reinvestigation regarding both diastereoselectivity and site-selectivity effects.

In this article the photodegradation of the diastereomeric KP/BSA complexes was studied by steady-state and laser flash photolysis. CD titration experiments were performed in order to determine the association constants relevant to the KP/BSA system, under various conditions. On the basis of the binding data, the photolysis quantum yields of the 1/1 and 2/1 diastereomeric complexes were estimated, shining some light on the site dependency of the KP photodecarboxylation in the protein matrix.

MATERIALS AND METHODS

Materials. S(+)-2-(3-benzoylphenyl)propionic acid (ketoprofen, KP), racemic KP, bovine serum albumin (99%, essentially globulin and fatty-acid

* To whom correspondence should be addressed: Istituto per la Sintesi Organica e la Fotoreattività, CNR, Via P. Gobetti 101, 40129 Bologna, Italy. Fax: ++39 051 639 9844; e-mail: monti@isof.cnr.it

† This paper is part of a special issue dedicated to Professor J. C. (Tito) Scaiano on the occasion of his 60th birthday.

Abbreviations: BSA, bovine serum albumin; CD, circular dichroism; HSA, human serum albumin; KP, 2-(3-benzoyl-phenyl)propionic acid (ketoprofen); NSAID, nonsteroidal antinflammatory drug; Trp, tryptophan; Tyr, tyrosine.

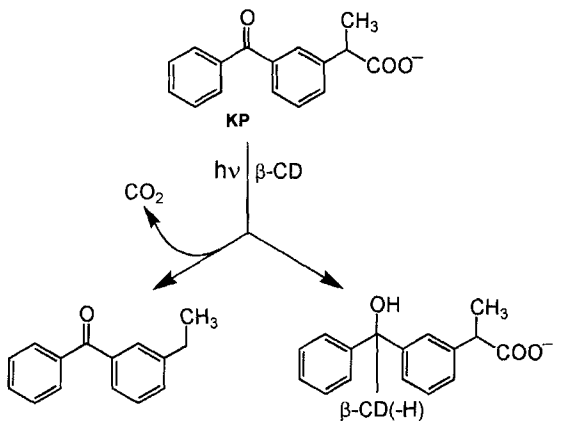

Scheme 1.

free) were purchased from Sigma-Aldrich (Milan, Italy). R(−)-2-(3-benzoylphenyl)propionic acid was prepared according to a biocatalytic procedure consisting of three sequential steps and exploiting lipase from *Candida antarctica*, of known R stereopreference, adsorbed on acrylic resin (Novozyme 435, Sigma-Aldrich). A detailed description of the preparation procedure has already been given (14).

Phosphate buffers of 0.01 or 0.1 *M* concentration at pH 7.4 were used as solvents for spectroscopic, steady-state and time-resolved photochemical measurements. The concentration of the buffer was chosen in the light of the concentration of KP. Water was purified by passage through a Millipore MilliQ system (Millipore SpA, Milan, Italy). All solvents used were HPLC grade.

Sample preparation. Identical aliquots of BSA were weighted and dissolved each in identical volumes of either buffer or a KP solution at the required concentration. The samples, gently stirred to complete protein dissolution, were carefully protected from ambient light during the manipulations in order to avoid photodegradation of KP, occurring in aqueous solutions at neutral pH with very high quantum yields (3). All the experiments were performed at a constant BSA content of either 1 mg/mL (1.5×10^{-5} *M*) or 16 mg/mL (2.4×10^{-4} *M*). The concentration of the buffer was either 0.01 or 0.1 *M*.

Spectroscopic measurements. All the measurements were performed at 25°C. Ultraviolet absorption spectra were recorded on a Perkin-Elmer λ49 spectrophotometer (Perkin Elmer, Milan, Italy) with 0.2 cm cells. CD spectra were obtained with a Jasco J-715 spectropolarimeter (Jasco-Europe srl, Modena, Italy) in cells of 2 cm and 0.2 cm path, for BSA concentrations of 1.5×10^{-5} and 2.4×10^{-4} *M*, respectively. The spectra were registered in the 290–400 nm range by using accumulation and time integration for improvement of signal-to-noise ratio.

Binding calculations. The assessment of the best complexation model and the determination of the association constants of the complexes were performed by global analysis of a series of CD spectra obtained at 10–12 different KP concentrations, with the use of the whole 290–400 nm wavelength range for the calculations. The computing program (SPECFIT/32, Spectrum Software Associates, Marlborough, MA) is based on singular value decomposition and nonlinear regression modeling by the Levenberg-Marquardt method and is commercially available. No equations were used, the procedure being completely numerical. The starting hypothesis was that the system might be described by contemporary presence of 1:1 and 2:1 KP:BSA complexes and free components. The CD spectra of the free KP enantiomers were introduced in the calculation as known data. The CD spectrum of the protein alone, dissolved in the buffer, was subtracted from the total CD spectrum of each of the KP/BSA mixtures, before analysis. No assumptions on the binding mechanism, that is, about presence or not of interdependency of binding sites or cooperativity in multiple binding, were introduced. The goodness of fit was judged on the basis of sum of squared residuals, residual distribution and standard deviation. The output consisted of the best association constants and the absolute spectra of the complexes.

Steady-state photolysis. Solutions of KP (1.5×10^{-5} *M* and 3×10^{-5} *M*) and BSA (1.5×10^{-5} *M*) in phosphate buffer were allowed to incubate in the dark for 20 min under gentle stirring. The samples were then degassed with a gentle nitrogen flow for 20 min and irradiated in 3 mL quartz cuvettes for different time lengths. The irradiated mixtures were filtered through a Millipore cutoff filter (Ultrafree-MC) to separate the protein from KP. After filtration, the filter was washed three more times with buffer, and the aqueous fraction solution was diluted to final volume of 6 mL. The percentage of unreacted drug was quantified through a LC-ESI-MS system (Hewlett-Packard, Milan, Italy) equipped with on-line photodiode-array detector (DAD) and a LiChro Cart RP-18 column (5 μm packing, 4 × 250 mm). The eluant was a mixture of CH_3OH:H_2O:CH_3COOH (58:42:2, vol:vol) operating at flow rate of 1 mL min^{-1} with an injection volume of 20 μL. Comparative experiments with a KP sample not incubated with BSA showed that almost 90% of the unreacted KP is separated from the BSA through the above filtration procedure. The only photoproduct detected was 3-ethylbenzophenone, but its quantum yield of formation was not addressed. Irradiations were performed with a Rayonet photoreactor equipped with black phosphorous lamps emitting in the range 320–390 nm with a maximum at 350 nm.

Nanosecond laser flash photolysis. The setup for the nanosecond absorption measurements was described previously (15). The minimum response time of the detection system was about 2 ns. The laser beam (Nd:YAG, operated at λ = 355 nm, 20 ns FWHM) was focused on a 3-mm-high and 10-mm-wide rectangular area of the cell and the first 2 mm in depth were analyzed at right-angle geometry. The incident pulse energies used were < 40 mJ/cm^2 (12 mJ/pulse). The bandwidth used in the spectrokinetic measurements was typically 2 nm (0.5 mm slit width). The spectra were reconstructed point by point from time profiles taken each 5–10 nm. The sample absorbance at 355 nm was 0.1–0.17 over 1 cm. Oxygen was removed by saturating the atmosphere above the solution by argon and gently stirring without bubbling. The solution, in a sealed cell of 1 cm path, was renewed after few laser shots. The temperature was 295 ± 2 K. Acquisition and processing of the absorption signals were performed by a homemade program with the use of Asyst 3.1 (Software Technologies, Inc.). Nonlinear fitting procedures by the least-square method were applied, and χ^2 and distribution of residuals were used to judge the goodness of the fit.

RESULTS

Binding studies. The binding constants of KP to BSA were determined by CD at two different BSA concentrations. Experiments were performed at BSA concentrations of 1 mg/mL (1.5×10^{-5} *M*) and 16 mg/mL (2.4×10^{-4} *M*) in phosphate buffer 0.01 and 0.1 *M*, respectively, at pH 7.4 and at 25°C, to match the conditions of the steady-state and flash-photolysis experiments (see below). Titration was performed with S(+)- and R(−)-KP in the KP/BSA molar ratio range 0.4–2.1. The intrinsic signal of the pure KP enantiomers in the region 290–400 nm was very weak, because of the flexibility of the benzophenone moiety promoting interconversion of chiral conformers (16), but increased substantially when BSA was present. The intrinsic θ signal of the protein, a tail of the intense negative band at 209/222 nm (17), was subtracted to better show the changes due to the formation of the associates. As an example of the experimental results, the set of CD spectra obtained for 1.5×10^{-5} *M* BSA with S(+)-KP as titrant is shown in Fig. 1a.

The full set of spectra was globally analyzed with the use of an iterative numerical procedure (see the Experimental section). The analysis afforded the stoichiometry of the most stable complexes and the values of the binding constants (Table 1). The best complexation model in the chosen molar ratio range was that with simultaneous presence of both 1:1 and the 2:1 KP/BSA complexes. The agreement between calculated and experimental ellipticity values was generally very good. The absolute CD spectra of the complexes for the S(+) enantiomer in $\Delta\Delta\varepsilon$ are shown in Fig. 1b. The spectra of the complexes, as expected, turned out to be independent of the BSA concentration used in the experiments. In the analysis of the sets of spectra relevant to the R(−)-enantiomer at 1.5×10^{-5} and 2.4×10^{-4} *M* BSA concentration, convergence in the minimization procedure was obtained by imposing as constraints

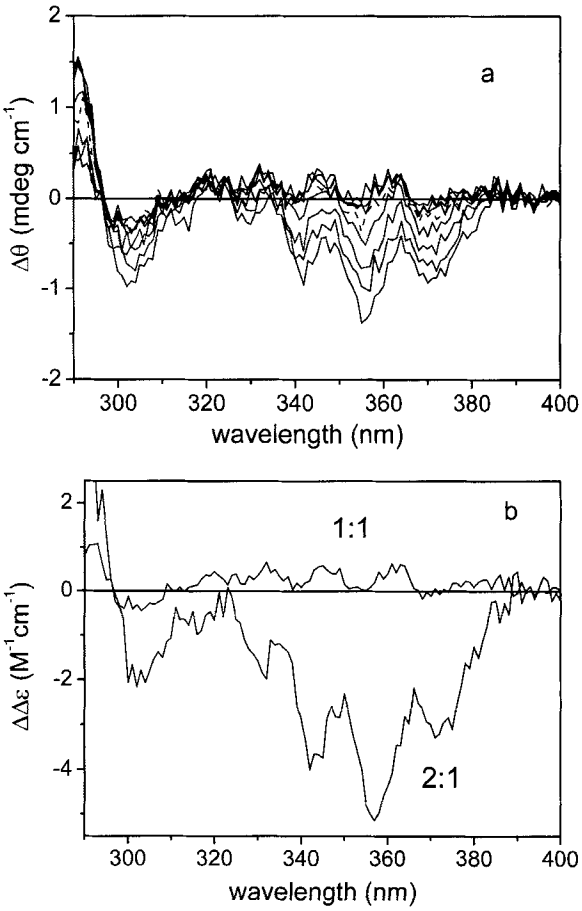

Figure 1. (a) Ellipticity changes ($\Delta\theta$) obtained by titration of BSA 1.5×10^{-5} *M* with S(+)-KP in the range 6×10^{-6} *M*–3.1×10^{-5} *M*. Phosphate buffer 0.01 *M*, pH 7.4, 25°C, cell 2 cm. The signal of BSA alone was subtracted. (b) Circular dichroism spectra in $\Delta\Delta\varepsilon$ of the S(+)-KP:BSA complexes obtained from global analysis of the experiment above.

the absolute CD spectra of the 1:1 and the 2:1 complexes, determined by global analysis of the experiment at 4.5×10^{-5} *M* BSA concentration (Fig. 2a,b) (14) *.

As expected on the basis of previous knowledge on KP binding to HSA (18), the equilibrium constants decrease on increasing the protein concentration.

Steady-state photolysis. The photodegradation of KP enantiomers in the BSA matrix was studied at 1.5×10^{-5} *M* BSA concentration, in 0.01 *M* phosphate buffer at pH 7.4, applying broad band irradiation with $\lambda_{irr} > 320$ nm (useful range 320–390 nm). Racemic KP was used as reference (quantum yield of photodegration $\Phi_{deg} = 0.75$, Reference 3). The photolysis course of the pure enantiomers was checked and was found to be identical to that of the racemic mixture of equal total concentration. In Figs. 3 and 4 the percentage of photolyzed KP is represented as a function of the irradiation time, for rac-KP and for KP/BSA mixtures with molar ratios 1/1 and 2/1, respectively. All the plots are linear (up to

* Convergence in the analyses with the R(−) enantiomer was generally more difficult, due to the similarity of the spectral shapes along with the titration, in the presence of noise at low BSA concentration and scattering of light at high BSA concentration. At intermediate BSA concentration the overall quality of the data was better and this likely favored mathematical convergence.

Table 1. Apparent binding constants of 1:1 (K_{11}) and 2:1 (K_{21}) KP:BSA complexes determined at different protein concentrations within KP/BSA molar ratio interval 0.4–2.1

	S(+)-KP		R(−)-KP	
BSA	Log K_{11}/M^{-1}	Log K_{21}/M^{-2}	Log K_{11}/M^{-1}	Log K_{21}/M^{-2}
1.5×10^{-5} *M*	5.7 ± 0.4	10.0 ± 0.5	6.3 ± 0.2	10.8 ± 0.3
4.5×10^{-5} *M**	5.3 ± 0.3	9.6 ± 0.3	5.1* ± 0.5	9.0 ± 0.4
2.4×10^{-4} *M*	4.0 ± 0.3	7.8 ± 0.5	4.1 ± 0.1	7.7 ± 0.2

* Experiment reported in Reference 14.

40–45% KP degradation) and can be directly compared, because the two reference courses were normalized to each other with respect to the KP concentration.

When we calculated the quantum yields, it was taken into account that, because of changes in the absorption spectra upon association of the drug to the protein, the amount of light absorbed in the KP/BSA mixtures and in the corresponding reference KP solutions was not the same. Considering the average absorbances in the 320–390 nm range (measured against the buffer in a 4 cm cell), the apparent quantum yields $\langle\Phi_{deg}\rangle$ for KP photodegradation at the two molar ratios were obtained from the slopes Π of the linear plots of Figs. 3

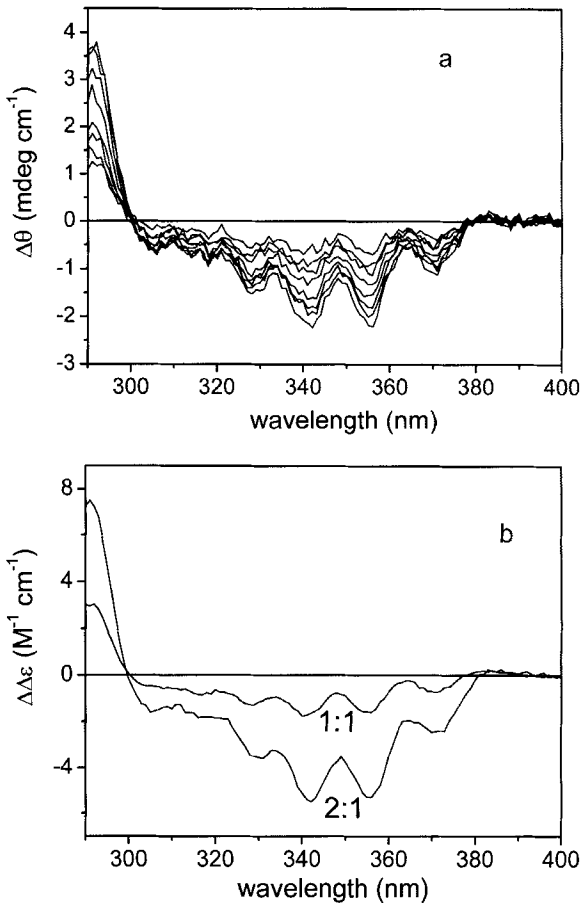

Figure 2. (a) Ellipticity changes ($\Delta\theta$) obtained by titration of BSA 1.5×10^{-5} *M* with R(−)-KP in the range 6×10^{-6} *M*–3.1×10^{-5} *M*. Phosphate buffer 0.01 *M*, pH 7.4, 25°C, cell 2 cm. The signal of BSA alone was subtracted. (b) Circular dichroism spectra in $\Delta\Delta\varepsilon$ of the R(−)-KP:BSA complexes obtained from global analysis of the experiment at BSA 4.5×10^{-5} *M*, from Reference 14.

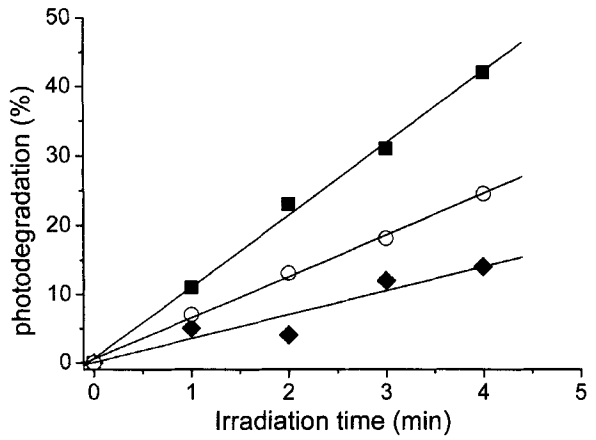

Figure 3. Photolysis course of S(+)- (◆) and R(−)-(○)KP/BSA mixtures in 1/1 molar ratio and of pure rac-KP (■), taken as standard, in phosphate buffer 0.01 *M*, pH 7.4, at 25°C, by irradiation at wavelengths $\lambda > 320$ nm. BSA and KP concentrations were both 1.5×10^{-5} *M*.

and 4. A detection limit of 0.1 for the degradation quantum yield was estimated in the used irradiation conditions.

Evaluation of the quantum yields for the individual KP complexes was performed on the basis of binding constants of Table 1. The slope Π for a mixture KP/BSA was first corrected for the percentage of light absorbed by the uncomplexed BSA molecules (concentration and molar absorption coefficient of free BSA were determined as described below) and the obtained $\Pi_{corr}^{KP/BSA}$ was considered to be proportional to a linear combination of the degradation quantum yield times the concentration times the ⟨ε⟩ of each KP species in solution. Equation 1 could be written:

$$(\Pi^{rac\text{-}KP})/(\Pi_{corr}^{KP/BSA}) = \langle\varepsilon_{KP}\rangle[KP]_{tot}\Phi_{deg}^{buffer}/(\langle\varepsilon_{KP}\rangle[KP]_{free}\Phi_{deg}^{buffer} + \langle\varepsilon_{11}\rangle[1:1]\phi_{deg}^{1:1} + \langle\varepsilon_{2:1}\rangle[2:1]\phi_{deg}^{2:1}) \quad (1)$$

The concentrations of free KP, free BSA, 1:1 complex, 2:1 complex were calculated at both 1/1 and 2/1 molar ratios on the basis of the equilibrium constants of Table 1. The average absorption coefficients ⟨ε⟩ in the 320–390-nm interval were obtained from the average total absorbances measured in the mixtures of S(+)- and R(−)-KP with BSA in 1/1 and 2/1 molar ratios and in the pure BSA and pure KP solutions. The two unknowns, that is, ϕ_{deg} of the 1:1 and of the 2:1 complexes, were determined for each enantiomer by using the two molar ratio conditions. Table 2 reports the experimental data and the results of the calculations. The individual ϕ_{deg}s of the KP complexes have to be considered as being approximate, because of uncertainty in the binding constants and possible errors in the ⟨ε⟩ evaluation.

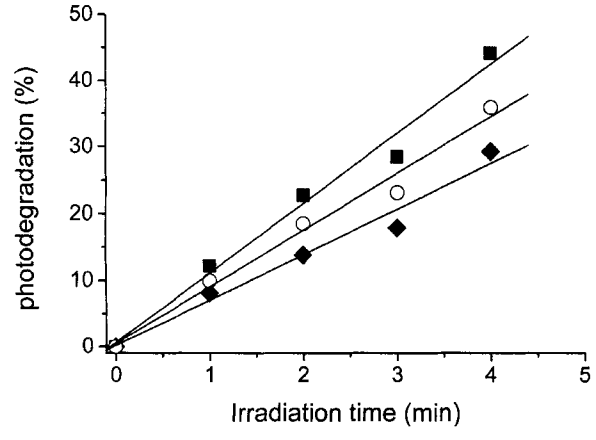

Figure 4. Photolysis course of S(+)- (◆) and R(−)-(○)KP/BSA mixtures in 2/1 molar ratio and of pure rac-KP (■), in phosphate buffer 0.01 *M*, pH 7.4 at 25°C, by irradiation at wavelengths $\lambda > 320$ nm. BSA was 1.5×10^{-5} *M*, KP was 3×10^{-5} *M*. The course for the rac-KP standard solution was normalized to that of Figure 3.

Table 2. Measured KP degradation rate Φ/% min^{-1} (from Figures 3 and 4) and apparent quantum yield $\langle\Phi_{deg}\rangle$ for 1/1 and 2/1 molar ratio conditions, at BSA 1.5×10^{-5} *M*, average molar absorption coefficients in the range 320–390 nm ⟨ε⟩ and quantum yields ϕ_{deg} of the 1:1 and 2:1 complexes. ⟨ε⟩ and ϕ_{deg} were calculated on the basis of K_{ij} of Table 1, according to the procedure described in the text

	$\Pi(\Pi_{corr})$/ % min^{-1}*	$\langle\Phi_{deg}\rangle$†	$\langle\varepsilon\rangle/M^{-1}$ cm^{-1} (320–390 nm)	ϕ_{deg} 1:1 complex	ϕ_{deg} 2:1 complex
Rac-, S(+)-, R(−)-KP	10.4	0.75	117		
BSA			285		
S (+)-KP/BSA					
1/1 molar ratio	3.5 (4.5)	0.09			
2/1 molar ratio	6.8 (7.2)	0.24			
S(+):BSA 1:1 complex			241	0.04	
S(+):BSA 2:1 complex			857		0.18
R(−)-KP/BSA					
1/1 molar ratio	6.0 (6.9)	0.16			
2/1 molar ratio	8.5 (8.6)	0.34			
R(−):BSA 1:1 complex			293	0.17	
R(−):BSA 2:1 complex			438		0.38

* Values in parentheses are corrected for the percentage of light absorbed by the free protein fraction, determined on the basis of the association constants of Table 1; see text.

† Experimental uncertainty ± 0.1; values calculated from uncorrected Π values.

Laser flash photolysis. Time-resolved experiments at λ_{exc} = 355 nm were performed with both enantiomers at KP/BSA molar ratios 1/1 and 2/1, in 0.1 *M* phosphate buffer at pH 7.4. Because of the low absorption coefficients, drug concentration was increased to 2.4×10^{-4} and 4.8×10^{-4} *M* and, correspondingly, BSA concentration was kept at 2.4×10^{-4} *M*.

No transients were generated by excitation of the protein alone. In the KP/BSA mixtures the difference spectra, taken 50 ns after the laser pulse, were characterized by two bands at 320–330 and 530 nm and by an intense tail extending beyond 650 nm. The spectral features were similar for both enantiomers. The relative intensity of the UV and Vis peaks turned out to be dependent on the molar ratio, with the 320–330 nm peak more important in the 2/1 condition; see Table 3 and Figs. 5 and 6 for the S(+)-KP enantiomer.

The transient absorption disappeared with biphasic kinetics in the microsecond time domain. The λ_{max} of both the UV and the visible bands did not change appreciably during time evolution. A small residual absorption survived at about 330 nm and remained constant up to several milliseconds. The decays were well described by biexponential functions (see insets of Figs. 5 and 6 and Table 3). Lifetimes (a "short" τ_s and a "long" τ_l) were found to be different for the two enantiomers and sensitive to the presence of oxygen: In deaerated solutions $\tau_s = 400 \pm 50$ ns and $\tau_l = 2.6 \pm$

Table 3. Flash photolysis at λ_{exc} = 355 nm of the KP/BSA system at molar ratios 1/1 and 2/1. Lifetimes, preexponential factors B_s and B_l of the short- and long-lived components; spectral data. Laser pulse energy 7.5 mJ

KP	molar ratio KP/BSA	τ_s/ns	τ_l/μs	B_s:B_l (%:%) 320–330 nm	520–530 nm	$\Delta A^{UV}/\Delta A^{Vis}$ (50 ns)
S(+)	1/1	400 ± 50	2.6 ± 0.5	62:38	66:34	1.6
	2/1			66:34	74:26	2.3
R(−)	1/1	600 ± 100	6.0 ± 0.5	43:57	45:55	1.6
	2/1			50:50	50:50	2.7

0.5 μs for S(+)- and τ_s = 600 ± 100 ns and τ_l = 6.0 ± 0.5 μs for R(−)-KP; in air-equilibrated solutions τ_s = 260 ± 40 ns and τ_l = 1.6 ± 0.1 μs for S(+)- and τ_s = 340 ± 40 ns and τ_l = 3.9 ± 0.2 μs for R(−)-KP. On the basis of these data the bimolecular rate constant for quenching by O_2 of the shorter-lived component appears to be ≈ 10^9 M^{-1} s^{-1}, whereas that of the longer-lived transient is about 1 order of magnitude lower.

By taking into account both the oxygen effect on τ_s and the absorption features of triplet KP in nonaqueous environments, known to be characterized by bands at 330 and 530 nm and microsecond lifetime (19), we assigned the early transient spectra to triplet species of KP bound in hydrophobic protein sites. We disregarded a KP ketyl radical assignement, because this latter in a nonaqueous medium was shown to have a maximum at 545–550 nm and insignificant absorption above 600 nm (5,9). The differences in the spectra between the 1/1 and 2/1 molar ratio conditions (Table 3) were attributed to the presence of different mixtures of triplet 1/1 and 2/1 KP/BSA complexes, each of them having specific spectral features. A higher contribution from the 2/1 complex apparently results in a more intense UV band. The differences in the lifetimes of the two enantiomers were consistent with a chemical/physical interaction of the ketone excited state with the environment, specifically determined by the chirality of the drug. The long-lived component was assigned to a further intermediate (see Discussion).

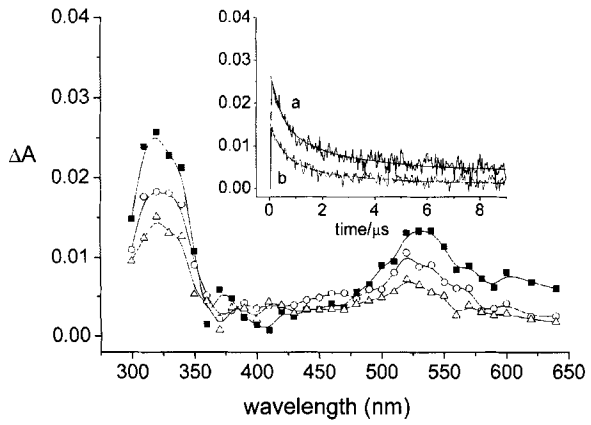

Figure 5. Difference absorption spectra generated after laser excitation at 355 nm of a deaerated solution of S(+)-KP/BSA in 1/1 molar ratio, in phosphate buffer 0.1 *M*, pH 7.4 at 25°C. BSA and KP concentrations were both 2.4 × 10^{-4} *M*, A_{355} = 0.11. Delays after pulse were 50 ns (■), 400 ns (○), and 840 ns (△). Inset: kinetic profiles at 320 nm (a) and 530 nm (b) and biexponential fits with ΔA_∞ = 0.006, B_s = 0.017, τ_s = 410 ns, B_l = 0.016, τ_l = 2.5 μs (a) and ΔA_∞ = 0.0015, B_s = 0.015, τ_s = 350 ns, B_l = 0.008, τ_l = 2.7 μs (b).

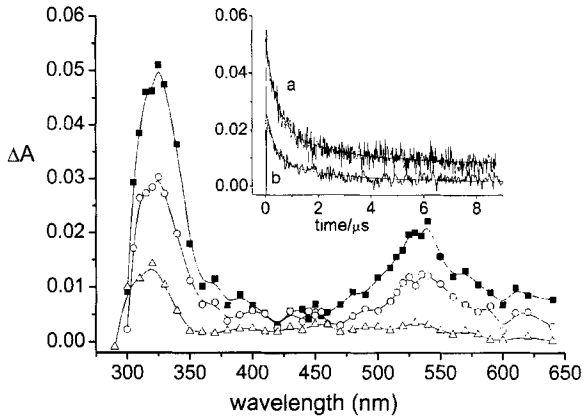

Figure 6. Difference absorption spectra generated after laser excitation at 355 nm of a deaerated solution of S(+)-KP/BSA in 2/1 molar ratio, in phosphate buffer 0.1 *M*, pH 7.4 at 25°C. BSA was 2.4 × 10^{-4} *M*, KP was 4.8 × 10^{-4} *M*, A_{355} = 0.16. Delays after pulse were: 50 ns (■), 425 ns (○), 3500 ns (△). Inset: kinetic profiles at 320 nm (a) and 530 nm (b) and biexponential fits with ΔA_∞ = 0.005, B_s = 0.020, τ_s = 400 ns, B_l = 0.008 τ_l = 2.7 μs (a) and ΔA_∞ = 0.0013, B_s = 0.012, τ_s =410 ns, B_l = 0.003, τ_l = 2.6 μs (b).

The photoreactivity of the free KP fraction was not in evidence. Indeed, in the spectra any absorption component around 580 nm with a lifetime of about 130 ns, which would be expected from the carbanion generated by photodecarboxylation of KP in a neutral aqueous medium (4,5) (see Scheme 2) was not distinguishable. This fact can be rationalized by the low fraction of the excitation light (≤25%) absorbed by unbound KP (whose concentration could be estimated on the basis of the relevant equilibrium

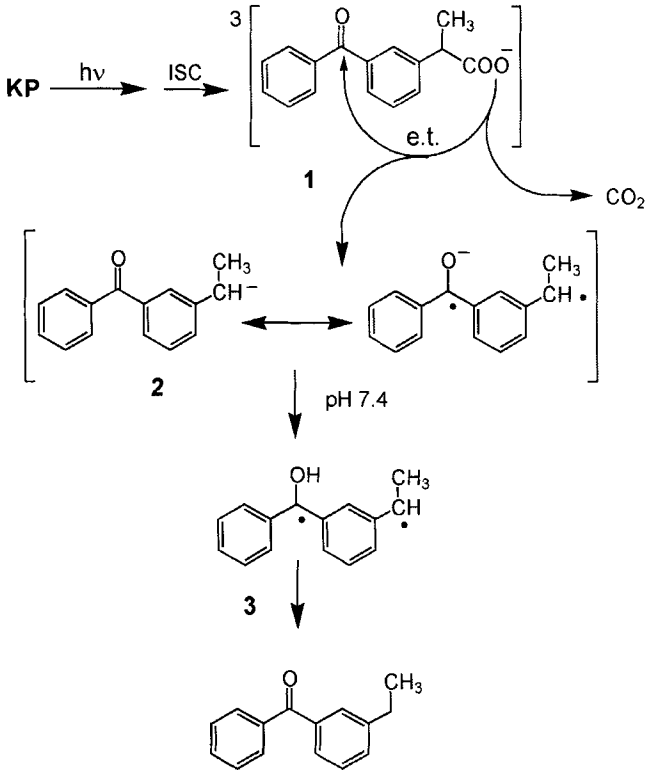

Scheme 2.

constants of Table 1). However, some shortening found in decay lifetimes at about 580–600 nm was consistent with a small contribution of the free carbanion in this region.

DISCUSSION

The photostability of KP appears to be substantially increased in the BSA matrix with respect to the aqueous solutions. The effect is greater at the 1/1 than at the 2/1 molar ratio and, in agreement with previous findings (13), is greater for the S(+) enantiomer. The degradation quantum yields of the various KP forms present in solution (Table 2) nicely account for the observed behavior. Indeed, ϕ_{deg} for the S(+) enantiomer, from a value of 0.75 in neutral aqueous medium (3), decreases by more than a factor of 10 in the 1/1 and by a factor of 4 in the 2/1 complex. The same trend is observed for the R(−) enantiomer, but here the protein exerts a lower protection (reduction of the ϕ_{deg}s was by factors of 4 and 2 in the 1/1 and 2/1 complexes, respectively).

These data can be discussed in more detail in the light of the results of a study, previously performed, of the time-resolved tryptophan fluorescence in the KP/BSA system (14), which indicated that the sites involved in the binding of KP enantiomers were Site I in Subdomain IIA and Site II in Subdomain IIIA (site names from Sudlow [20] and domain assignment from the X-ray structure of the homologue HSA [21,22]), the 1:1 complexation of R(−)-KP occurring in Subdomain IIA and that of S(+)-KP in Subdomain IIIA. Thus for each enantiomer the site of highest affinity turns out to be the most protective. Additional occupancy of the second site, that is, Site II in Subdomain IIIA for R(−)- and Site I in Subdomain IIA for S(+), is responsible for increased photolability. One would be tempted to hypothesize additivity in the photoreactivity of sequentially bound KP molecules. However, independent photobehavior in the two sites cannot be *a priori* assumed, because the involved Subdomains IIA and IIIA share a common interface (21,22).

The most striking results from the laser flash photolysis measurements were that (a) the triplet state of KP was observable in the submicrosecond time domain; and (b) the primary intermediate of KP decarboxylation, that is, the carbanion, was not evidenced. In some respects these results parallel those obtained in the β-cyclodextrin cavity, where the KP triplet, undetectable in the nanosecond time domain in water (4,5), was shown to reach a 100 ns lifetime (7). The lengthening of the KP triplet lifetime in the apolar cyclodextrin interior was attributed to the slowing down of the rate of the intramolecular electron transfer promoting the release of carbon dioxide (see Scheme 2). Because the main photoreaction taking place in the BSA matrix is still photodecarboxylation (13 and this work), a similar scenario seems to apply fairly well also in the protein. Here electron transfer from the carboxylate group to the aromatic carbonyl moiety can be made inefficient, first because the negatively charged group is involved in an electrostatic interaction with a positive $-NH_3^+$ of the protein (this was deduced on the basis of the completely different CD spectra of the KP methylester derivative complexed to BSA itself [14]), second, because the aromatic carbonyl group, constrained by the rigid, apolar microenvironment of the protein, cannot easily stabilize the carbanion by accommodating the negative charge made available by the loss of the CO_2 fragment.

However, the triplet seems to remain in the photoreactive state for both enantiomers. Indeed it is unlikely that the singlet excited state may play a role in this system, because intersystem crossing in nonaqueous media was shown to be unitary (19) and was also believed to be such in water (4,6). Moreover triplet formation does not seem to compete with the photoreaction, because the intensity of the triplet absorption in 1/1 and 2/1 conditions does not show any decrease when the photodegradation quantum yields substantially increase (compare the spectra in Figs. 5 and 6).

As to the kinetic properties of the triplet, longer lifetimes were exhibited by the more photolabile enantiomer. Moreover, for a given enantiomer similar lifetimes were found at molar ratios that strongly differentiate in the overall photoreactivity. This is consistent with the photoreaction not being the main process to determine the triplet decay. Other deactivation paths must take place and be influenced by stereospecific interactions.

The lack of the carbanion maximum at 580 nm (4,5) in the spectra of samples with high fractions of KP bound to BSA (for example, in Figs. 5 and 6 the fractions of bound S[+]-KP were about 70 and 60%, respectively),† can be tentatively attributed to a fast protonation step occurring upon decarboxylation and preventing any accumulation of this transient species within the protein matrix. In this case the oxygen-sensitive species with maximum at about 320 and 530 nm (see spectra at longer delays in Figs. 5 and 6) with lifetime 2.6 and 6.0 μs with S(+) and R(−)-KP, respectively, can be assigned to the triplet neutral biradical **3** (see Scheme 2). Accordingly, the spectral and kinetic properties of this transient are in agreement with those attributed to **3** in water at neutral pH (4,6). However, this assignment remains tentative, because we are not certain that the long-lived transient absorption pertains exclusively to the photodecarboxylation path (see below). Within the above interpretative scheme, the action of the protein is that of inducing a modification of the intramolecular reactivity of KP enantiomers and/or providing a way for a fast protonation step upon photofragmentation, finely tuning these effects *via* the specific site interactions.

Decarboxylation could not be the only photoprocess of KP in the BSA matrix. Covalent photobinding was indeed observed in Subdomain IIIA of HSA with a racemic mixture of KP (9). Furthermore, it is a matter of fact that, in the analytical runs following the photolysis of the KP/BSA solutions, the amount of 3-ethylbenzophenone recovered did not account for all the disappeared KP. ‡ Because excited ketone chromophores are known to participate in electron transfer reactions involving phenols and indoles (23,24) or in stereoselective hydrogen abstraction processes (25), such processes could take place with partners like tyrosine and tryptophan, which are located in Site II of Subdomain IIIA (Tyr 409) and in Site I of subdomain IIA (Trp 212) (14) or with other close-lying H-donating residues.

In this way a long-lived radical pair containing an amino-acid radical and a ketyl radical center should be generated. This species could, by recombining in the protein cage, convert back to the starting molecules or lead to covalent photoadducts. Ketyl radicals derived from benzophenone-like molecules are known to have a visible absorption not significantly extending beyond 600 nm (27), somewhat redshifted with respect to that of the corresponding

† Because of the low absorption coefficients, as already noted in the Results section, free KP does not absorb more than 25% of excitation light.

‡ However, because of the much higher hydrophobicity of this photoproduct when compared to KP, we cannot exclude that the discrepancy in the mass balance could be attributable, at least in part, to an incomplete extraction of the photoproduct itself from the BSA matrix by the experimental procedures used.

triplet state and with slight dependence on the medium polarity (28); actually, as already mentioned, the KP ketyl radical in a nonaqueous medium has a maximum at 545–550 nm (5,19). On the other hand, a Trp(-H)$^{\bullet}$ radical has λ_{max} = 330 and 520 (29) and the Tyr(-H)$^{\bullet}$ phenoxyl radical has λ_{max} = 405 nm (30). Given the compatibility of the absorption features of the above radicals with the spectra at long delays, we cannot exclude that some such radical species might contribute to the absorption. Thus the KP reductive photochemistry in the BSA matrix could be in part similar to that of benzophenone in the same environment, where the ketyl and the partner radical, confined in the protein cage, survived by retaining geminate character, on the microsecond timescale (31). Similarly, long-lived radical pairs resulting from caged photochemistry were detected in the triplet-state mediated photoaddition of KP to β-cyclodextrin (7) and in analogous reactions of other benzophenone derivatives in cyclodextrin cavities (15).

Finally, it worth recalling that triplets decaying on the submicrosecond–microsecond timescales, quenched by oxygen, are expected to form singlet oxygen, superoxide radical, or both, by energy and/or electron transfer. Studies addressing these matters, which are of great importance for the photosensitizing action of KP against cell substrates, are under way in our laboratories.

Acknowledgements—This work was performed with the financial support of CNR (Italy) within the frame of the project "Ligand–receptor interactions: model spectroscopic, photophysical and conformational studies," and the financial support of MIUR (Rome, Italy).

REFERENCES

1. Bosca, F., M. L. Marin and M. A. Miranda (2001) Photoreactivity of the nonsteroidal anti-inflammatory 2-arylpropionic acids with photosensitizing side effects. *Photochem. Photobiol.* **74**, 637–655.
2. Bosca, F., M. A. Miranda, G. Carganico and D. Mauleon (1994) Photochemical and photobiological properties of ketoprofen associated with the benzophenone chromophore. *Photochem. Photobiol.* **60**, 96–101.
3. Costanzo, L. L., G. De Guidi, G. Condorelli, A. Cambria and M. Fama (1989) Molecular mechanism of drug photosensitization. II—Photohemolysis sensitized by ketoprofen. *Photochem. Photobiol.* **50**, 359–365.
4. Monti, S., S. Sortino, G. De Guidi and G. Marconi (1997) Photochemistry of 2-(3-benzoylphenyl)propionic acid (ketoprofen). A picosecond and nanosecond time resolved study in aqueous solution. *J. Chem. Soc. Faraday Trans.* **93**, 2269–2275.
5. Martinez, L. J. and J. C. Scaiano (1997) Transient intermediates in the laser flash photolysis of ketoprofen in aqueous solutions. Unusual photochemistry for the benzophenone chromophore. *J. Am. Chem. Soc.* **119**, 11066–11070.
6. Borsarelli, C. D., S. E. Braslavsky, S. Sortino, G. Marconi and S. Monti (2000) Photodecarboxylation of ketoprofen in aqueous solution. A time resolved laser-induced optoacoustic study. *Photochem. Photobiol.* **72**, 163–171.
7. Monti, S., S. Sortino, G. De Guidi and G. Marconi (1998) Supramolecular photochemistry of 2-(3-benzoylphenyl)propionic acid (ketoprofen). A study in the β-cyclodextrin cavity. *New J. Chem.* 599–604.
8. Dormán, G. and G. Prestwich (1994) Benzophenone photophores in biochemistry. *Biochemistry* **33**, 5661–5673.
9. Chuang, V. T. G., A. Kuniyasu, H. Nakayama, Y. Matsushita, S. Hirono and M. Otagiri (1999) Helix 6 of subdomain IIIA of human serum albumin is the region primarily photolabeled by ketoprofen, an arylpropionic acid NSAID containing a benzophenone moiety. *Biochim. Biophys. Acta* **1434**, 18–30.
10. Moser, J., Z. Sarabia, H. Minter, W. W. Lovell and G. M. J. Beijersbergen van Henegouwen (2000) Photobinding of ketoprofen *in vitro* and *ex vivo*. *J. Photochem. Photobiol. B* **58**, 37–45.
11. Lahoz, A., D. Hernandez, M. A. Miranda, J. Perez-Prieto, I. M. Morera and J. Castell. (2001) Antibodies directed to drug epitopes to investigate the structure of drug–protein photoadducts. Recognition of a common photobound substructure in tiaprofenic acid/ketoprofen cross-photoreactivity. *Chem. Res. Toxicol.* **14**, 1486–1491.
12. Hutt, A. J. and J. Caldwell (1984) The importance of stereochemistry in the clinical pharmacokinetics of the 2-arylpropionic acid non steroidal anti-inflammatory drugs. *Clin. Pharmacokinet.* **9**, 371–373.
13. Festa, C., N. Levi-Minzi and M. Zandomeneghi (1996) Photochemistry in biological matrices: binding site photoreactivity of ketoprofen in serum albumins and chiral discrimination. *Gazz. Chim. Ital.* **126**, 599–603.
14. Monti, S., F. Manoli, S. Sortino, R. Morrone and G. Nicolosi (2005) Binding of a chiral drug to a protein: an investigation of the 2-(3-benzoyl-phenyl)propionic acid/bovine serum albumin system by circular dichroism and fluorescence. *Phys. Chem. Chem. Phys.*, **7**, 4002–4008.
15. Monti, S., N. Camaioni and P. Bortolus (1991) Photochemistry in a cyclodextrin cavity. Primary processes in the photoreduction of 3- and 4-benzoylpyridine studied by laser flash-photolysis. *Photochem. Photobiol.* **54**, 577–584.
16. Zandomeneghi, M. (1995) Circular dichroism of ketoprofen complexed to serum albumins: conformational selection by the protein: a novel optical purity determination technique. *Chirality* **7**, 446–451.
17. For a review on serum albumins see T. Peters Jr. (1985) Serum albumin. *Adv. Protein Chem.* **37**, 161–245.
18. Dubois, N., F. Lapicque, M. Abiteboul and P. Netter (1993) Stereoselective protein binding of ketoprofen: effect of albumin concentration and of the biological system. *Chirality* **5**, 126–134.
19. Cosa, G., L. J. Martinez and J. C. Scaiano (1999) Influence of solvent polarity and base concentration on the photochemistry of ketoprofen: independent singlet and triplet pathways. *Phys. Chem. Chem. Phys.* **1**, 3533–3537.
20. Sudlow, G., D. J. Birkett and D. N. Wade (1976) Further characterization of specific drug binding sites on human serum albumin. *Mol. Pharmacol.* **12**, 1052–1061.
21. He, X. M. and D. C. Carter (1992) Atomic structure and chemistry of human serum albumin. *Nature* **358**, 209–215.
22. Carter, D. C. and J. X. Ho (1994) Structure of serum albumin. *Adv. Prot. Chem.* **45**, 153–203.
23. Prieto, J. P., A. Lahoz, F. Bosca, R. Martinez-Manez and M. A. Miranda (2004) Stereodifferentiation in the decay of triplets and biradicals involved in intramolecular hydrogen transfer from phenols or indoles to π, π* aromatic ketones. *J. Org. Chem.* **69**, 374–381.
24. Prieto, J. P., F. Bosca, R. E. Galian, A. Lahoz, L. R. Domingo and M. A. Miranda (2003) Photoreaction between 2-benzoylthiophene and phenol or indole *J. Org. Chem.* **68**, 5104–5113.
25. Miranda, M. A., L. A. Martinez, A. Samadi, F. Bosca, and I. M. Morera (2002) Stereoselective intramolecular hydrogen abstraction by a chiral benzophenone derivative. *Chem. Commun.* 280–281.
26. Jovanovic, S. V. and S. Steenken (1992) Substituent effects on the spectral, acid-base, and redox properties of indolyl radicals: a pulse radiolysis study. *J. Phys. Chem.* **96**, 6674–6679.
27. Scaiano, J. C., E. B. Abuin and L. C. Stewart (1982) Photochemistry of benzophenone in micelles. Formation and decays of radical pairs. *J. Am. Chem. Soc.* **104**, 5673–5679.
28. Land, E. J. (1968) Extinction coefficients of triplet-triplet transitions. *Proc. R. Soc. A* **305**, 457–471.
29. Bent, D. V. and E. Hayon (1975) Excited state chemistry of aromatic aminoacids and related peptides. III. Tryptophan. *J. Am. Chem. Soc.* **97**, 2612–2619.
30. Bent, D. V. and E. Hayon (1975) Excited state chemistry of aromatic aminoacids and related peptides. I. Tyrosine. *J. Am. Chem. Soc.* **97**, 2599–2606.
31. Mohat, N., F. L. Cozens, T. Hancock-Chen, J. C. Scaiano, J. McLean and J. Kim (1998) Magnetic field effects on the behavior of radicals in protein and DNA environments. *Photochem. Photobiol.* **67**, 111–118.